Nanochem Res 3(1): 36-49, Winter and Spring 2018

RESEARCH PAPER

Sunlight-driven efficient photocatalytic and antimicrobial studies of microwave-assisted Ir-doped TiO_2 nanoparticles for environmental safety

Dasari Ayodhya*, Perka Shyam and Navaneetha Nambigari

Department of Chemistry, Osmania University, Hyderabad, Telangana State, India

ARTICLE INFO

Article History:
Received 7 January 2018
Accepted 13 February 2018
Published 1 March 2018

Keywords:
Antimicrobial Activity
Chlorinated Phenols
Ir-doped TiO_2 NPs
Microwave-Assisted Method
Photodegradation

ABSTRACT

A simple, low-cost and an eco-friendly synthesis of Ir-doped titanium dioxide nanoparticles (TiO_2 NPs) with an anatase phase by the microwave-assisted method using an aqueous solution of titanium tetra-isopropoxide (TTIP) and iridium (III) chloride monohydrate. The synthesized Ir-doped TiO_2 NPs were characterized by using various spectro-analytical techniques for the confirmation of NPs. The photocatalytic activity of the synthesized Ir-doped TiO_2 NPs has been evaluated by taking 2-chlorophenol (2-CP), 4-chlorophenol (4-CP), 2,4-dichlorophenol (2,4-DCP) and 2,4,6-trichlorophenols (2,4,6-TCP) as model water contaminant pollutants under sunlight irradiation. The photocatalytic conversion is approximately 84.24%, 81.22%, 76.01% and 72.11% of 2-CP, 4-CP, 2,4-DCP and 2,4,6-TCP respectively, by using the synthesized Ir-doped TiO_2 NPs. The efficient photocatalytic degradation was observed in the degradation of 2-CP in 60 min of sunlight irradiation. The rate equation of photocatalytic degradation mechanism was followed pseudo-first order kinetics. Finally, the screening of antimicrobial activity by paper disc method against few bacteria, such as Escherichia coli (E. coli), Pseudomonas aeruginosa (P. aeruginosa), Bacillus subtilis (B. subtilis) and Staphylococcus aureus (S. aureus) and fungi such as Aspergillus niger (A. niger) and Candida albicans (C. albicans), showed that the prepared Ir-doped TiO_2 NPs have the prominent results.

How to cite this article
Ayodhya D, Shyam P, Nambigari N. Sunlight-driven efficient photocatalytic and antimicrobial studies of microwave-assisted Ir-doped TiO_2 nanoparticles for environmental safety. Nanochem Res, 2018; 3(1): 36-49. DOI: 10.22036/ncr.2018.01.005

INTRODUCTION

Recently, the use of solar irradiation-based semiconductors, dealing with the environmental problems, is drawing a lot of attention. Reducing the size of the semiconductors will modify their physical, chemical, or biological properties, especially under irradiation [1]. Among these various semiconductors at the nanoscale, TiO_2 NPs have been used widely to remove polluted organic chemicals and bacteria in the water because this material has high specific surface area and chemical stability. At present, antibiotics offered in the marketplace are primarily organic. Along with technical development, however, inorganic antibiotics have gradually replaced them. As a novel inorganic antibacterial material, TiO_2 NPs have received increasing attention for their stable, long-lasting properties, as well as their safety, low cost and broad-spectrum antibiosis [1-3]. As the production of TiO_2 and its use in consumer products increases, its release into the environment is increased, as a result of spills, use of products, or post-consumer degradation of the material. Predicted environmental concentrations of TiO_2 NP in water are on the order of parts per billion, with expected environmental loads as high as

* Corresponding Author Email: *ayodyadasari@gmail.com*

10-60 lakh tons in the next 10 years [4-6]. The accumulation of NP in the environment is likely to be non-uniform [5], with higher concentrations in near-shore waters which are more impacted by run-off, wastewater discharge, and proximity to human populations. TiO_2 NP concentrations of 1-100 mg/L are known to have deleterious effects on the environment. Thus, there is a need to understand the environmental impact of these NP. The photocatalytic properties of metal oxide NP (e.g., TiO_2, CeO_2 and ZnO) are well known [7-8], and TiO_2 NP have been exploited in a wide range of photocatalytic applications including coated nanocomposites in sunscreens for ultraviolet (UV) protection and in 'green' technology cement that actively purify the air of pollutants [9]. In aqueous media, TiO_2 NP can produce radicals when activated by UV light. The radicals, in turn, can damage microbes and provide an antimicrobial property being utilized by medical, food and water-treatment industries [10].

The photocatalysts in photocatalytic process, especially those with high photocatalytic activity and strong stability under visible light have been regarded as capable materials for applications in solar energy conversion and treatment of wastewater [11-12]. Although TiO_2 is the most explored photocatalyst so far [13], the wide energy gap (3.2 eV) of TiO_2 has stalled its sufficient utilization of sunlight [14]. Therefore, the development of novel and more efficient visible-light-driven photocatalysts are still urgently needed from the viewpoint of solar energy conversion. TiO_2 is a wide band gap semiconductor corresponding to radiation in the near UV range (< 387 nm). Upon the absorption of UV energy, TiO_2 particles will form an electron-hole (e^-/h^+) pairs in the conduction band and valence band, respectively. The use of high energy UV light is not only costly but also can be hazardous. Therefore, the use of visible light active materials has recently drawn the attention of the researchers. The sunlight is most abundantly available, renewable and clean source of energy, which is composed of less than ~50 % of visible radiation and less than ~5 % of UV radiation [15]. To extend the spectral response of TiO_2 to the visible region, many modification methods have been investigated, including surface modified using various stabilizers and capping agents. Preparation of TiO_2 NPs using green technologies is advantageous over chemical agents due to their less environmental consequences, cost-effectiveness.

Many organic pollutants (chlorinated phenols) have been found in different water resources from chemical industries. Chlorophenols (CPs) have found wide use in pesticides, herbicides, disinfectants, wood preservatives, personal care formulations, dyestuff intermediates, and many other products, and they are also substantial by-products of wood pulp bleaching with chlorine [16]. CPs is poorly biodegradable with a half-life that can exceed some years in organic sediments. However, growing knowledge about the toxicities and environmental fates of specific chlorinated phenols has made governments regulate these compounds [17-18]. CPs have been found in at least 166 of the 1467 National Priorities List sites, and 4 of them are listed as priority pollutants, including 2-CP, 4-CP, 2,4-DCP, and 2,4,6-TCP, which are present in the environment in significant quantities. Moreover, except for 2-CP, 2,4,6-TCP and 2,3,4,6-tetrachlorophenol (2,3,4,6-TeCP), have been classified as group 2B environmental carcinogens by the International Association for Research on Cancer (IARC) [19]. Since the intermediate products originating from CPs degradation might be more toxic and cause secondary pollution, it is crucial to determine the intermediates and their associated toxicity. Therefore, it is essential to develop highly efficient and reliable technologies for their removal.

Herein, we report a way for the microwave-assisted synthesis of Ir-doped TiO_2 NPs in the green synthetic route by using an aqueous solution of iridium (III) chloride monohydrate and TTIP as titanium precursor. The synthesized Ir-doped TiO_2 NPs are characterized by various physicochemical techniques. The remarkable photocatalytic activity was observed for the degradation of chlorinated pollutants such as 2-CP, 4-CP, 2,4-DCP and 2,4,6-TCPs by the synthesized Ir-doped TiO_2 NPs. The degradation efficiency as a rate of conversion is also studied under sunlight irradiation. The rate of degradation is followed by the pseudo-first order kinetics through Langmuir-Hinshelwood model. The antimicrobial activity of the synthesized Ir-doped TiO_2 NPs shows prominent results.

EXPERIMENTALS

Methods and Materials

Titanium tetra isopropoxide (TTIP, 97%, Merck, India), iridium chloride monohydrate, isopropanol (99%, SD-Fine chemicals, India) and chlorophenols (2-CP, 4-CP, 2,4-DCP and 2,4,6-TCP) were

purchased from Merck, India. Double distilled water was used throughout the experiment.

Microwave-assisted preparation of Ir-doped TiO_2 NPs

The Ir-doped TiO_2 NPs were prepared using the simple microwave-assisted method. For the synthesis of Ir-doped TiO_2 NPs, the round bottom flask containing 10 mL of 0.25 M of titanium tetraisopropoxide (TTIP) in 90 mL isopropanol with constant stirring at room temperature to get a clear solution. 5 mL of 0.05 M of iridium chloride monohydrate solution was prepared and slowly added to the above solution with constant stirring for 20 min at 35 °C. These solutions were mixed together under an inert atmosphere and then heated to 50 °C for 1 h to get a clear solution. After 2 hours of continuous stirring, the precipitation of reaction mixture was formed. The precipitate was subjected to microwave irradiation for 5 min in a domestic microwave oven (Input 900 W, 250 MHz, LG Company) with on-off cycle (20 sec on to 40 sec off). Then, the formed Ir-doped TiO_2 NPs was acquired by centrifugation at 5000 rpm for 15 minutes. Then, the centrifuged particles were washed with ethanol and again subjected to centrifugation at 3000 rpm for 10 minutes. Separated Ir-doped TiO_2 NPs were dried, grinded, and calcinated at 500 °C in a muffle furnace for about 2 hours. The calcinated pure Ir-doped TiO_2 nanopowder was collected and used for the further analytical techniques.

Characterization techniques

The powder X-ray diffraction (XRD) spectra was recorded on a X'pert Pro powder X-ray diffractometer (Netherland) using the CuKα radiation (λ=0.15406 nm). The UV-Vis diffuse reflectance spectra (UV-Vis DRS) was recorded on a Shimadzu 3600 spectrophotometer in the spectral range of 200-800 nm. The morphology and particle size of the synthesized Ir-doped TiO_2 NPs were characterized by using a Transmission electron microscopy (TEM) on Tecnai G2 and the microscope was operated at 200 kV. Samples were prepared by dispersing the powder in double distilled water. Images were recorded by depositing few drops of suspension on a carbon coated 400 mesh Cu grid. The solvent was left to evaporate before imaging. SEM images of the prepared Ir-doped TiO_2 NPs were obtained using ZEISS EVO18 electron microscope. FTIR spectra on KBr pellet were measured on a Shimadzu spectrophotometer in the range of 4000-400 cm^{-1}. The fluorescence spectrum was measured with an RF-5301PC spectrofluorometer (Shimadzu, Japan). The thermal behavior and degradation of the Ir-doped TiO_2 NPs were investigated by thermogravimetric analysis in the range of 100 to 1000 °C at a heating rate of 10 °C min^{-1} under the nitrogen atmosphere.

Photocatalytic degradation of chlorophenols

The photocatalytic activities of the prepared Ir-doped TiO_2 NPs were evaluated by the degradation of 2-CP, 4-CP, 2,4-DCP and 2,4,6-TCP solutions under natural sunlight irradiation. All of the experiments were carried out under similar conditions on sunny days at times between 11.00 a.m. and 2.30 p.m. All photocatalytic experiments were applied at ambient temperature (28-38 °C). 0.05 g photocatalyst was added to 50 mL of 30 mg/L 2-CP, 4-CP, 2,4-DCP and 2,4,6-TCP solutions. Before the sunlight irradiation, the suspensions were magnetically stirred for 60 min to reach the adsorption-desorption equilibrium. At the given time interval, 3 mL aliquots were sampled and filtered with a micropore membrane. Simultaneously, the filtrates of phenol solutions at different conditions were analyzed by recording variations of the CPs peak area. The UV-Vis absorption spectrophotometer (UV-3600 spectrophotometer, Shimadzu) was adopted for analysis of 2-CP, 4-CP, 2,4-DCP and 2,4,6-TCP degradation with irradiation time. The sample with a volume of 20 µL was used as injection volume and concentrations of 2-CP, 4-CP, 2,4-DCP and 2,4,6-TCPs were evaluated by UV detector at wavelengths 290, 295, 287 and 310 nm, respectively. The photocatalytic degradation was calculated as follows:

$$\% D = \frac{A_o - A_t}{A_o} \times 100 \quad (1)$$

where D is the degradation efficiency, A_0 is the initial concentration of CPs and A_t is the concentration of CPs after irradiation in selected time interval.

Antibacterial activity

The synthesized Ir-doped TiO_2 NPs with different amounts (10 µL to 50 µL) were screened for in-vitro antibacterial activity against two Gram-negative bacteria such as *Escherichia coli* (ATCC 25922), *Pseudomonas aeruginosa* (ATCC

27853) and two Gram-positive bacteria such as *Staphylococcus aureus* (ATCC 25923) and *Bacillus subtilis* (MTCC 121) bacterial strains by paper disc method. Briefly, all cultures were routinely maintained on NA (nutrient agar) and incubated at 37 °C for overnight. The culture was centrifuged at 1000 rpm, pellets were re-suspended, and volume of 0.1 ml diluted bacterial culture suspension was spread uniformly with the help of spreader on NA plates. Wells of 6 mm diameter were punched into the agar medium and loaded with prepared NPs. Antibiotic disc; ampicillin (100 mg/disc) and solvent were used as positive and negative control, respectively. The plates were then incubated for 24 h at 37 °C and the resulting zones of inhibition (mm) were measured.

Antifungal activity

All cultures were routinely maintained on sabouraud dextrose agar (SDA) and incubated at 28 °C. The prepared Ir-doped TiO_2 NPs with different amounts (10 µL to 50 µL) were screened for their in-vitro antifungal activity against the fungi, *A. niger*, and *C. albicans* were performed by growing the culture in SDA broth at 37 °C for overnight. The volume of 0.1 ml of diluted fungal culture suspension was spread with the help of spreader on SDA plates uniformly. Sterile 6 mm discs were impregnated with the test samples and the wells of 6 mm size were cut and loaded with sample. Antibiotic disc, ketoconazole (10 µL/disc) was used as positive control. *A. niger* and *C. albicans* plates were incubated at 37 °C for 24–48 h and antifungal activity was determined by measuring the diameters of the inhibition zone (mm).

RESULT AND DISCUSSION

UV-Vis DRS analysis

UV-Vis DRS was used to determine particle size and the band gap of prepared Ir-doped TiO_2 NPs. UV-Vis DRS measurement is one of the most important methods to reveal the optical properties of TiO_2 samples. The UV-Vis DRS of the Ir-doped TiO_2 NPs is displayed in Fig. 1. The energy band gap of Ir-doped TiO_2 NPs was calculated using the equation: $E_g = hc/\lambda$, where h is Planck's constant; c is the velocity of light and λ is wavelength (in nm). The band gap of 3.54 eV at wavelength 351 nm corresponds to absorption peak. It can be seen that there was a significant shift of the absorption edge towards visible region for Ir-doped TiO_2 NPs. The band gap of Ir-doped TiO_2 NPs shows as 3.54 eV, it is a large deviation from the bulk TiO_2. The increase in the band gap compared to that of TiO_2 bulk is attributed to the quantum size effect. Based on the DRS results, blue shift is indicative of the charge transfer between Ir^{3+} and TiO_2 conduction band and valence band when compared with the pure TiO_2 NPs. As the number of electron-hole pairs on the surface of TiO_2 increases, the photocatalytic activity increases [20]. The apparent large blue shift of the observed absorption indicates that the NPs are within the quantum confinement regime, in which a blue shift in absorption is often expected with decreasing particle size.

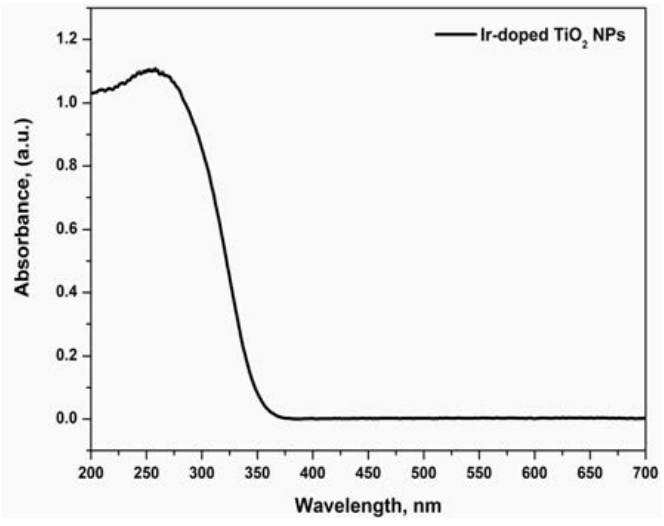

Fig. 1: UV-Vis DRS of Ir-doped TiO_2 NPs

PL analysis

The PL spectroscopy is the direct method for probing the electronic transition of nanomaterials. The study of transfer behavior of photo excited electron-hole pairs in the semiconductors and the rate of recombination is carried out by PL spectra [21]. The PL spectrum of the synthesized Ir-doped TiO_2 NPs is shown in Fig. 2. It shows the emission peak in the range of 425-465 nm after doping of Ir^{3+} ions into the TiO_2 NPs. The peak at 438 nm appeared in the PL spectrum. The appeared peaks correspond to a radiative transition of the excited electrons from occupied d-band to the higher state of Fermi level of Ir-doped TiO_2 NPs. The PL intensities of Ir-doped TiO_2 NPs were lower in comparison to those of reported TiO_2 NPs. It is observed due to changes in the electronic structure of Ir^{3+} containing TiO_2 NPs. Lower PL intensity indicates the delay in the rate of recombination and thus obtained photocatalytic activity is higher for Ir-doped TiO_2 NPs [22].

FTIR analysis

The FTIR spectra of the synthesized Ir-doped TiO_2 NPs were analyzed in the wave number range of 4000-600 cm^{-1} and are given in Fig. 3. Many absorption bands belong to the organic groups such as OH and C-C were appeared. In FTIR spectrum

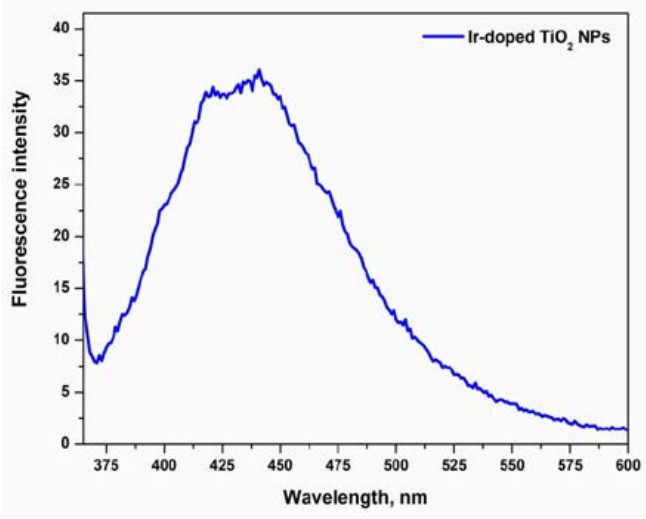

Fig. 2: Photoluminescence spectra of Ir-doped TiO_2 NPs

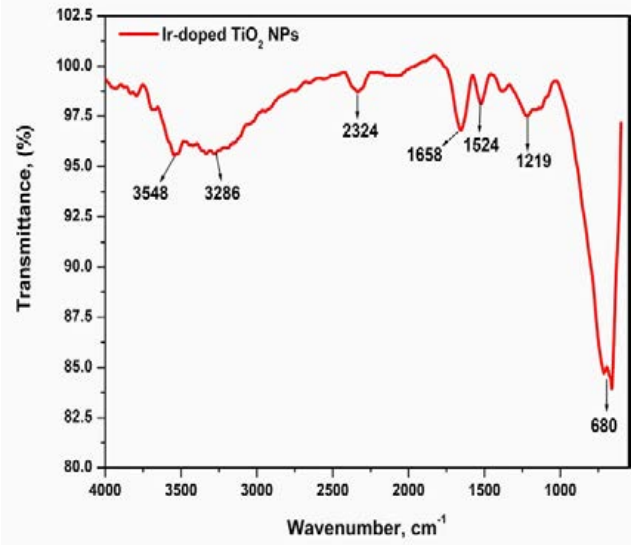

Fig. 3: The FTIR spectrum of Ir-doped TiO_2 NPs

of Ir-doped TiO_2 NPs, the broad peak appeared between 3800 to 3000 cm^{-1} was attributed to stretching hydroxyl (O-H), representing the water as moisture. The other peaks at 1658 cm^{-1} were indicated to stretching of titanium carboxylate, formed from TTIP and ethanol as precursors [23]. The peak between 724 and 645 cm^{-1} was assigned to the Ti-O stretching bands. In FTIR spectrum of Ir-doped TiO_2 NPs in the range of about 680 cm^{-1} is the Ti-O bending mode of vibrations which confirms the formation of metal-oxygen bonding [24]. Similarly, the broad band centered at 3286 and 1524 cm^{-1} was respectively attributed to stretching and bending vibrations of O-H of adsorbed water on the surface of TiO_2 which plays an important role in photocatalytic activity [25]. The peaks between 2941 and 2324 cm^{-1} are assigned to C-H stretching vibrations of alkene groups. A broad absorption band between 600 and 1000 cm^{-1} is attributed to the vibration of Ti-O-Ti association in TiO_2 NPs. In general, the conformation of the formation of doped TiO_2 NPs when compared to the pure TiO_2 NPs is the changes in intensity and position of the bands shifted towards the lower wave number after doping [26]. Only the strong absorption between 800 and 650 cm^{-1} was remained, which was attributed to the formed Ir-doped TiO_2 NPs.

XRD analysis

The formation of Ir-doped TiO_2 NPs was analysed by the powder X-ray diffraction measurements and are shown in Fig. 4. In the XRD analysis, five diffraction peaks at 24.8º, 37.4º 47.6º, 53.8º, and 62.2º obtained, have planes (101), (004), (200), (105) and (204), respectively, of the tetragonal body-centred titanium dioxide (JCPDS No. 86-1156). Very high anatase content is observed for the as-synthesized nanoparticles compared to the reference sample (99.7% of anatase, Aldrich). Indeed, no rutile peaks were found. This is due to the heat treatment at 450 °C which is known to produce high anatase content. Zhang et al. chose this calcination temperature because anatase has a better photocatalytic activity due to the higher electron-hole pair lifetime compared to rutile. It attributes the difference of activity, between anatase and rutile, to the direct/indirect band gap behavior of the phases [27]. Indeed, it was shown that anatase behaves as an indirect semiconductor; thus, electron de-excitation from the conduction band to the valence band is forbidden by selection rules. Hence, electron-hole lifetime is higher with anatase while rutile acts as a direct semiconductor with a lower carrier lifetime. The average particle size of Ir-doped TiO_2 NPs was estimated 10-15 nm which was calculated by Scherer's formula. The broadening of diffraction peak gradually increases, suggesting a systematic decrease in the grain size. Smaller crystallite size redounds to photogenerated carriers shifting to the surface of photocatalyst and prevents the recombination of the charge carriers, which, in turn improves the photocatalytic activity [28].

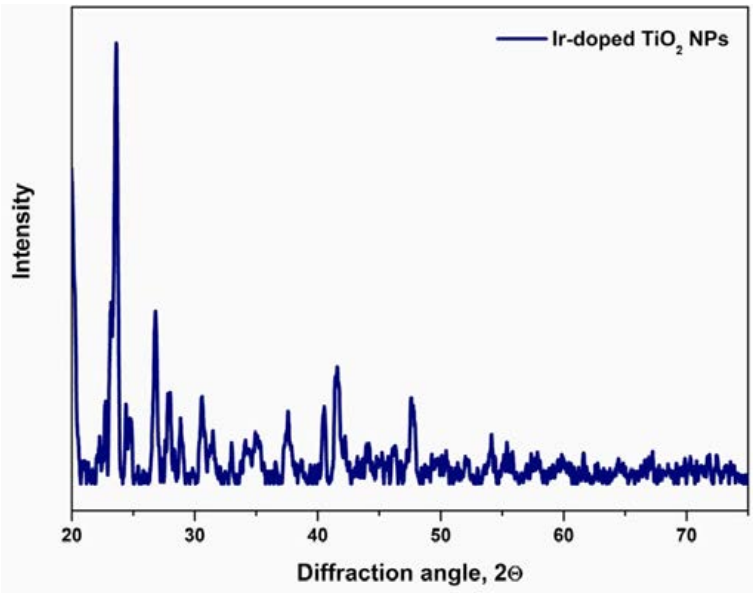

Fig. 4: Powder XRD pattern of Ir-doped TiO_2 NPs

SEM and TEM analysis

To know the morphological information of Ir-doped TiO_2 NPs, SEM and TEM techniques were carried out. Figs. 5 and 6 represent the SEM and TEM images of the synthesized Ir-doped TiO_2 NPs. SEM image of the sample indicates that the particles are nearly uniform size nano-domain and the particles vary in their shape with some agglomeration. The SEM with EDX images confirmed the spherical and bubble morphology of the prepared Ir-doped TiO_2 NPs. From the TEM image, the particle size of Ir-doped TiO_2 NPs is in the range of 10-20 nm which are in good agreement with XRD results. The decrease in the particle size of the TiO_2 is related to the nucleation mechanism in the growth process. To find out the elemental composition present in Ir-doped TiO_2 NPs, EDX recorded in the binding energy region of 0-10 keV. The number of well-defined peaks in the spectrum clearly supports the presence of Ti, O and Ir in the NPs. In the spectrum, no other peaks were detected which confirm the purity of nanomaterial. The atomic % of Ti, O and Ir are 32.51, 62.47 and 5.02, respectively. This indicates that the material formed is non-stoichiometric, with oxygen deficiency, which leads to the best performance for photocatalytic activity [29].

Thermal analysis

Fig. 7 shows TGA curve of Ir-doped TiO_2 NPs after drying at 100 °C for 4 h. Three main stages of TGA curve of TiO_2 sample according to the heat profile were observed in the range of 100-1000 ^{0}C. The temperature increases from 100 to 250 °C as the first stage, which is assigned to remove the remaining ethanol, water and about 32% weight loss occurred. Temperature range of 310 to 420 °C, is attributed to the decomposition of the organic compounds completely with about 9.02 % weight was lost [30]. The amorphous precursor was converted to anatase phase as the temperature increases from 425 to 500 °C. The TiO_2 anatase was transferred to rutile phase between 550 to 600 °C [31]. There is gradually weight loss up to 78.27% on TGA curve up to 1000 °C indicating that decomposition of TiO_2 precursor is completed.

Photocatalytic activity

Photocatalytic degradation of chlorinated phenols

The presence of CPs in aquatic environments has caused severe environmental pollution problems. In CPs, 2-CP, 4-CP, 2,4-DCP and 2,4,6-TCPs are typical phenolic substances that have been used as an intermediate in making insecticides, herbicides, preservatives, antiseptics, disinfectants and other organic compounds [32] and 2,4,6-TCP is particularly of environmental interest owing to its mutagenicity and carcinogenicity [33]. Traditional wastewater treatment techniques consist of activated carbon adsorption and biological digestion. Each of these techniques has limitations and disadvantages. For activated carbon, adsorption only involves the phase transfer of pollutants without decomposition thus introduces another pollution problem [34]. On the other hand, in biological treatment, the decomposition

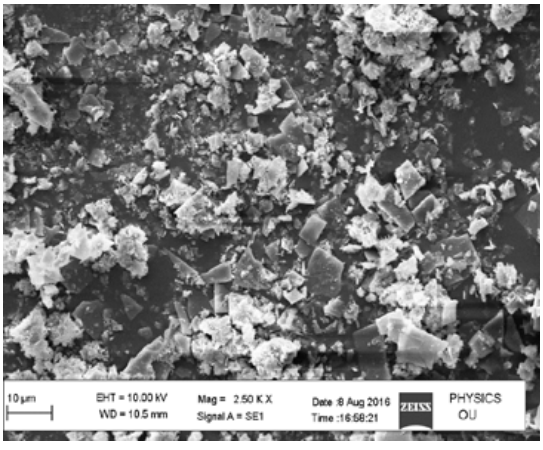

Fig. 5: SEM image of Ir-doped TiO_2 NPs

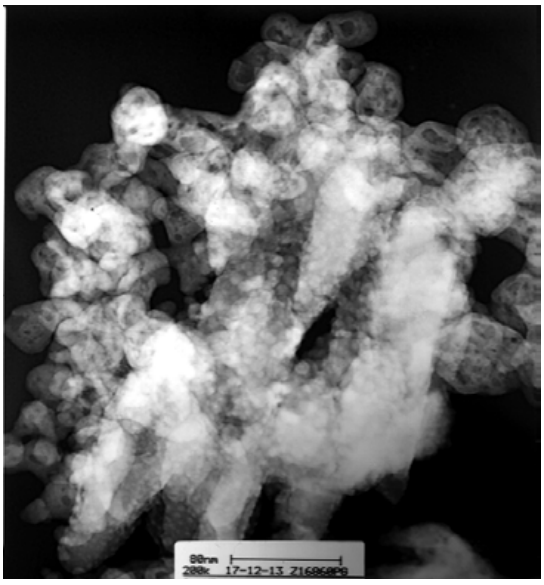

Fig. 6: TEM image of Ir-doped TiO_2 NPs

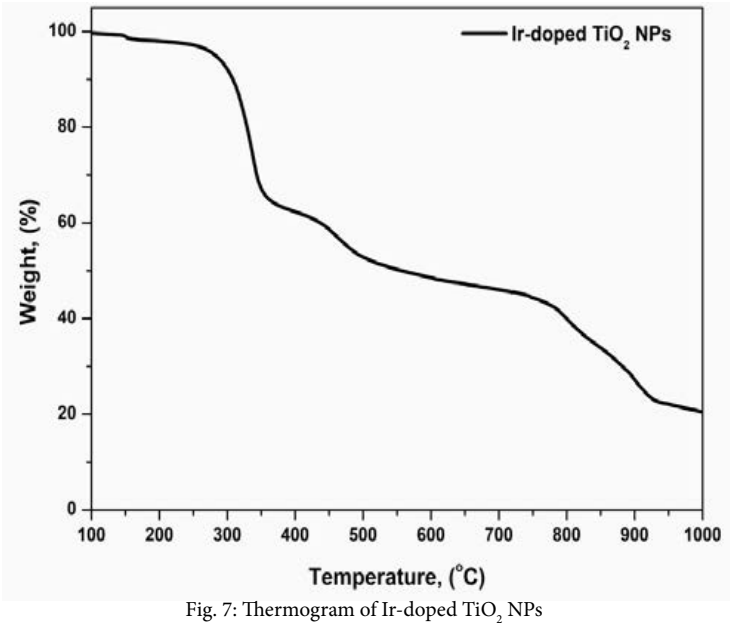

Fig. 7: Thermogram of Ir-doped TiO_2 NPs

of many CPs has proven inefficient since CPs resist to biodegradation within an acceptable time period and tend to accumulate in sediments [35]. The CPs do not undergo direct sunlight photolysis in the natural environment since they only absorb light below 290 nm [36]. Therefore, the advanced oxidation processes (AOP) appears to be a good method for destruction the toxic pollutants into nontoxic substances. Photocatalytic oxidation reactions are initiated when a photon of higher energy level or equal to the band gap energy is absorbed by a TiO_2 catalyst promoting an electron (e^-) from the valence band to the conduction band with simultaneous generation of a positive hole (h^+) in the valence band. One possible mechanism for this change in the photodegradation efficiency is as follows; by irradiation of the Ir-doped TiO_2, Ir^{3+} ions work as electron scavengers which may react with the superoxide species and prevent the holes-electrons (h^+/e^-) recombination and consequently increase the efficiency of the photooxidation. The mechanism of radical generation ($^{\bullet}OH$ and $^{\bullet}O_2^-$) is presented as follows [37]:

$$TiO_2 + h\nu \rightarrow TiO_2 (e^- + h^+) \quad (2)$$

$$H_2O + TiO_2 (h^+) \rightarrow TiO_2 + {}^{\bullet}OH + H^+ \quad (3)$$

$$O_2 + TiO_2 (e^-) \rightarrow TiO_2 + {}^{\bullet}O_2^- \quad (4)$$

$$Ir^{3+} + O_2^- (ads) \rightarrow Ir^{2+} + O_2 (ads) \quad (5)$$

To confirm the degradation of CPs due to photocatalysis, the sample of Ir-doped TiO_2 NPs tested as an adsorbent of these pollutants. Fig. 8 shows the UV-Vis absorption spectra of 2-CP, 4-CP, 2,4-DCP and 2,4,6-TCP in the absence of Ir-doped TiO_2 NPs as adsorbent at the maximum wavelength is 290, 295, 287 and 310 nm, respectively. The removal of 2-CP, 4-CP, 2,4-DCP and 2,4,6-TCP slightly decreased the absorption at the corresponding wavelengths in 60 min of sunlight irradiation. On the other side, Ir-doped TiO_2 NPs acted as an adsorbent for the removal of 2-CP, 4-CP, 2,4-DCP and 2,4,6-TCP. In this process, it is observed that the absorption intensity of the band at the corresponding wavelengths produced by the solution after adsorption with Ir-doped TiO_2 NPs is high in comparison with the band of only chlorinated phenols, indicating that under these conditions Ir-doped TiO_2 NPs adsorb molecules of CPs; however, the solution shows a light yellow colour, indicating that the adsorption process may produce some by-products, since it cannot degrade the benzene ring of the CPs. The interaction between the two compounds in water may lead to derivatives and by-products of CPs, corroborated by the yellow color of the solution and the increment in the absorption of the corresponding band at 225 nm for the benzene ring. Thus, this effect indicates that CPs are adsorbed via a link in the Ir-doped TiO_2 NPs by C–Cl linkages, with more than 80% of the CPs ultimately removed.

As mentioned before, a common characteristic of the presence of by-products generated by CPs, as the result of degradation process, is the yellow coloration of the solution, which indicates that intermediates are generated; however, if the final solution is transparent, it indicates that by-products generated are not excessive. Compounds such as hydroquinone and benzoquinone give a yellow color to the final solution of a treated CPs. The characteristic bands of CPs (290, 295, 287 and 310 nm) disappear independently in the spectra of Ir-doped TiO_2 NPs in the photocatalyst tests; it is standard to calculate the removal percentage with the band at 225 nm, which is the distinguishing

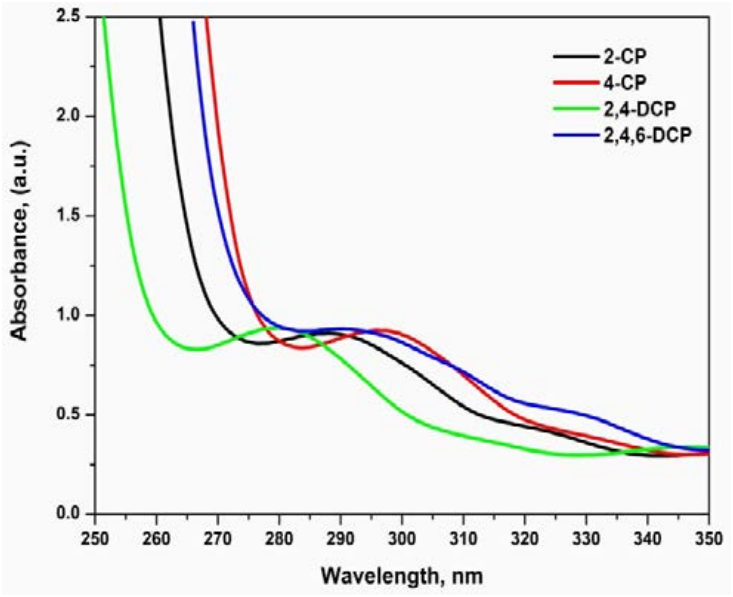

Fig. 8: UV-Vis absorption spectra of 2-CP, 4-CP, 2,4-DCP and 2,4,6-TCP

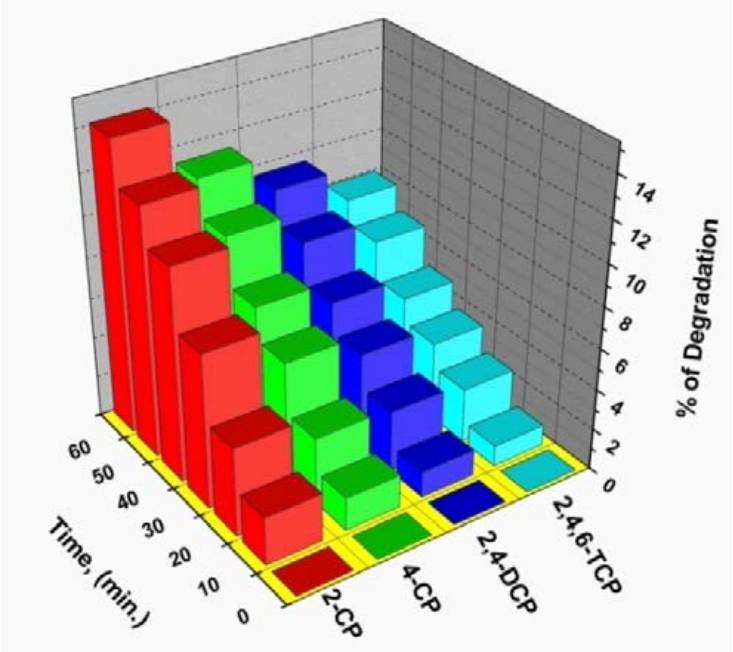

Fig. 9: The photocatalytic degradation efficiencies of 2-CP, 4-CP, 2,4-DCP and 2,4,6-TCP in the absence of Ir-doped TiO_2 NPs under sunlight irradiation

band for this quantification [38-39]. The enhanced photocatalytic activity for Ir-doped TiO_2 NPs could be attributed to the ability to capture and transport electrons and to promote charge separation. It is known that the higher separation efficiency of electron-hole pairs will enhance photocatalytic activity and results in a large number of holes participating in the photocatalytic process [40]. Degradation of 2-CP, 4-CP, 2,4-DCP and 2,4,6-TCPs, using TiO_2 as photocatalysts activated in UV zone supported in different materials such as activated carbon, silica, and zeolite have been reported [41-42]. Based on this data we developed a new synthetic route of Ir-doped TiO_2 NPs for the photocatalytic degradation of CPs in under sunlight irradiation. It is an industrial application of this method recommended because of the simple modification, high-efficiency removal and prevention of the environment pollution.

Degradation mechanism and efficiency

In order to avoid excess use of photocatalyst, it is essential to find out the optimum quantity of photocatalyst for better photodegradation of CPs. The effect of catalyst loading on the degradation of CPs was checked under sunlight irradiation by using optimal parameters of the concentration of CPs and amount of Ir-doped TiO_2 NPs are identical. It is seen that, initially, degradation efficiency increases with increase in the irradiation time. The photodegradation mechanism of 2-CP, 4-CP, 2,4-DCP and 2,4,6-TCP involves the photodissociation of the C-Cl bond in CPs has been reported using UV laser excitation [39]. The photochemical reaction is the first stage in the C-Cl bond cleavage of CPs, with the subsequent decomposition of the intermediate ion or radical [40]. It is important to consider the band at the corresponding wavelengths which define the generation of intermediate compounds in the progression of CPs degradation. Figs. 9 and 10 show the 3D-bar diagrams of photocatalytic degradation efficiencies of 2-CP, 4-CP, 2,4-DCP and 2,4,6-TCP in the absence and presence of Ir-doped TiO_2 NPs under 60 min of sunlight irradiation. It clearly indicates more than 12% and 80% of photodegradation of CPs in the absence and presence of Ir-doped TiO_2 NPs, respectively. It indicates that the wavelength emitted by the used light is capable of activating OH groups in the solution, causing oxidation due to air trapped in the reactor where the reaction takes place and breaking the C-Cl bonds present in CPs. In principle, the photodegradation rate of CPs is affected by not only the active sites but also the photoabsorption of the catalyst used [43]. It is important to remember that the by-products in many cases are more toxic so

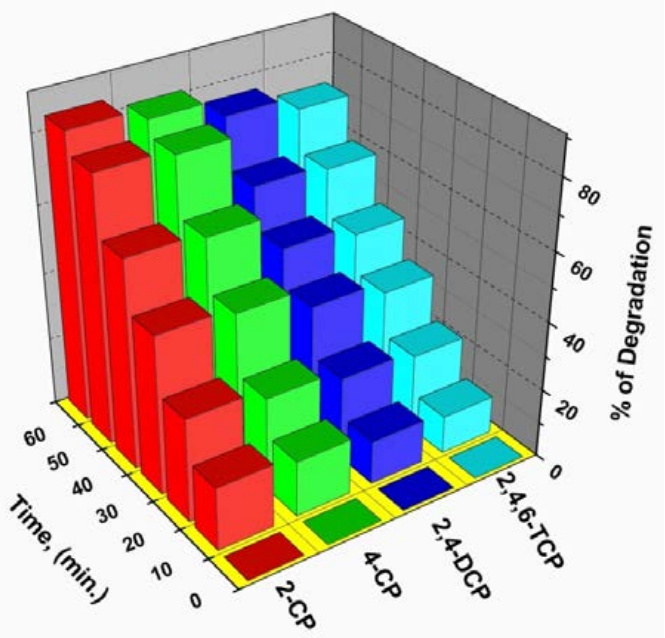

Fig. 10: The photocatalytic degradation efficiencies of 2-CP, 4-CP, 2,4-DCP and 2,4,6-TCP in the presence of Ir-doped TiO_2 NPs under sunlight irradiation

that the photolysis process alone is not a sufficient method to completely degrade CPs.

Kinetic analysis

The kinetics of photocatalytic reactions of CPs using Ir-doped TiO_2 NPs in aqueous solution follows Langmuir-Hinshelwood model:

$$\text{Rate} = -dC/dt = K_{app}\, C, \; (K_{app} = k_r K_a) \quad (6)$$

where k_r is the rate constant and K_a is the adsorption equilibrium constant. When the adsorption of CPs on Ir-doped TiO_2 catalyst is relatively weak, the K_a and C are insignificant, and the equation can be simplified to the first-order kinetics with an apparent rate constant ($K_{app} = k_r K_a$).

$$\ln [C_0/C_t) = k_{app}\, t \quad (7)$$

The apparent rate constant (k_{app}) evaluated by using above-equation and pseudo-first-order kinetics of CPs degradation was obtained. The degradation efficiencies, apparent rate constants and half-life period values are reported in Table 1 to show the wide-ranging comparison. The kinetic plots were drawn for the photocatalytic degradation of CPs in the absence and presence of Ir-doped TiO_2 NPs and it follows the pseudo-first order kinetics (Figs. 11 and 12). The overall photodegradation rate decreases on order of 2-CP > 4-CP > 2,4-DCP > 2,4,6-TCP. These results indicate that the rate constant reduces in sequence from 2-CP to 2,4,6-TCP, which illustrates the difficult attack on the 2,4,6-TCP ring by HO• radical because it is an electrophilic reagent. The 2,4,6-TCP ring has lower solubility property (higher hydrophobicity) than that of 2-CP, 4-CP and 2,4-DCP. From the previous

Table 1: The calculated photodegradation efficiency, rate constants and half-life period values of 2-CP, 4-CP, 2,4-DCP and 2,4,6-TCP in the absence and presence of Ir-doped TiO_2 NPs under sunlight irradiation

S.No.	Sample	Degradation efficiency, (%)	Rate constant, (min^{-1})	Half-life period, (min.)	R^2
1	2-CP	14.21	0.0048	144.43	0.99
2	4-CP	11.34	0.0041	169.02	0.99
3	2,4-DCP	9.65	0.0035	198.01	0.98
4	2,4,6-TCP	8.05	0.0028	247.48	0.99
5	2-CP+Ir-TiO_2 NPs	84.24	0.0214	32.38	0.99
6	4-CP+ Ir-TiO_2 NPs	81.22	0.0195	35.54	0.98
7	2,4-DCP+ Ir-TiO_2 NPs	76.01	0.0168	41.25	0.97
8	2,4,6-TCP+ Ir-TiO_2 NPs	72.11	0.0142	48.81	0.97

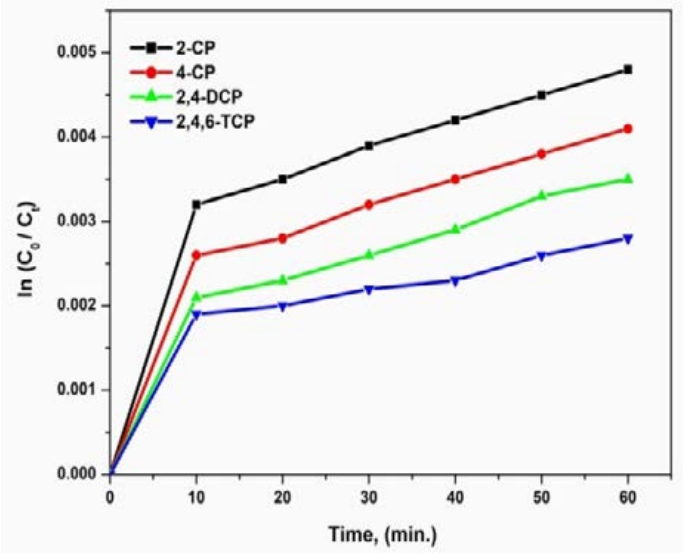

Fig. 11: The kinetic plots of the photocatalytic degradation of 2-CP, 4-CP, 2,4-DCP and 2,4,6-TCP in the absence of Ir-doped TiO_2 NPs under sunlight irradiation

results, the degradation rate of CPs is faster when chlorophenol hydrophobic property is decreased and increases the solubility [44].

Antimicrobial activity

The synthesized Ir-doped TO_2 NPs with various amounts (10 µL to 50 µL) were screened for the in-vitro antibacterial activity against Gram- positive *B. subtilis, S. aureus* and Gram-negative *E. coli, P.aeruginosa*, and antifungal activity against *A. niger* and *C. albicans* and the relevant data are presented in Table 2 and Fig. 13. The diameter of the zone of inhibition (mm) was used to compare the antimicrobial activity of the tested sample with the standards (Ampicillin and Ketaconazole were used as standard drugs for antibacterial and anti-fungal activity, respectively). The results revealed that nanoparticles have varying degrees of inhibitory effects on the growth of bacterial and fungal strains that may be due to the effect of the metal ion on the cell metabolism. The 50 µL amount of Ir-doped TiO_2 NPs showed remarkably good anti-bacterial activity against *B. subtilis* and *E. coli* with zone diameter 14 and 11 mm, respectively, while moderate activity against *S. aureus* and *P. aeruginosa* with zone diameter 10 and 8 mm, respectively. The synthesized Ir-doped TiO_2 NPs (10 µL to 50 µL) were also screened for their antifungal activity against *A. niger,* and *C. albicans*. Interestingly the prepared sample exhibited prominent antifungal activity against the all fungi with significant inhibition zone diameter. The significant antimicrobial activity of the nanoparticles can be attributed to the fact that the lipid membranes that surround the cell favor the passage of only the lipid-soluble materials which

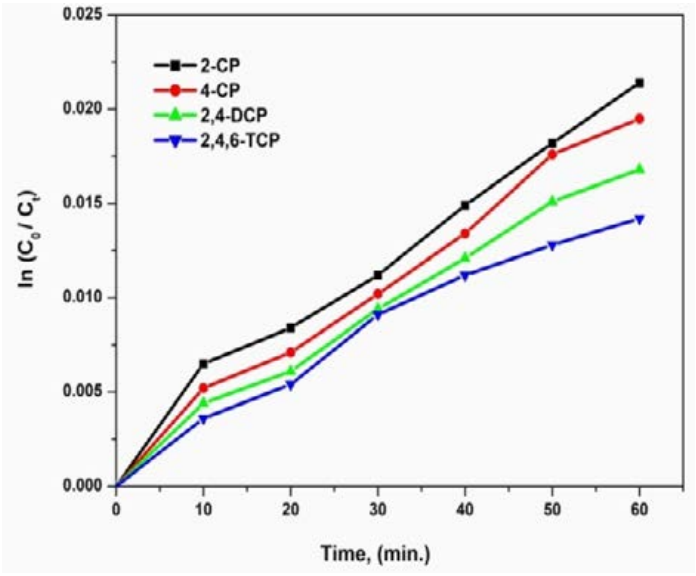

Fig. 12: The kinetic plots of the photocatalytic degradation of 2-CP, 4-CP, 2,4-DCP and 2,4,6-TCP in the presence of Ir-doped TiO_2 NPs under sunlight irradiation

Table 2: The antibacterial and antifungal activities with varying amount of the prepared Ir-doped TiO_2 NPs

Sample	*Amount of sample*	*Zone of inhibition, mm*					
		B.subtilis	*S.aureus*	*E.coli*	*P.aeruginosa*	*A.niger*	*C.albicans*
Ir-doped TiO_2 NPs	10 µL	08±0.4	06±0.6	06±0.6	04±0.2	06±0.3	03±0.5
Ir-doped TiO_2 NPs	20 µL	09±0.4	07±0.6	08±0.2	05±0.2	08±0.3	05±0.5
Ir-doped TiO_2 NPs	30 µL	11±0.4	08±0.6	09±0.2	06±0.2	09±0.3	06±0.5
Ir-doped TiO_2 NPs	40 µL	13±0.4	09±0.6	10±0.2	07±0.2	10±0.3	08±0.5
Ir-doped TiO_2 NPs	50 µL	14±0.4	10±0.6	11±0.2	08±0.2	12±0.3	09±0.5
Ampicillin	10 µL	16±0.6	14±0.2	17±0.3	15±0.4	-	-
Ketoconazole	10 µL	-	-	-	-	16±0.5	14±0.4

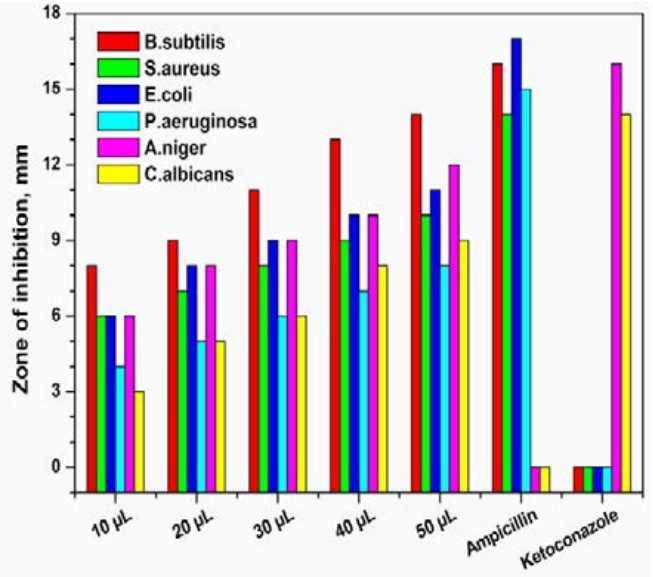

Fig. 13: The antibacterial and antifungal activity of the different amounts (10 µL to 50 µL) of synthesized Ir-doped TiO_2 NPs

makes liposolubility as an important factor that controls the antibacterial activity.

CONCLUSION

In summary, the microwave-assisted method was used for the preparation of Ir-doped TiO_2 NPs and characterized using different techniques such as XRD, SEM and TEM for structure and morphology studies. Optical properties of the synthesized Ir-doped TiO_2 NPs were characterized using UV-Vis DRS and PL. XRD analysis showed that the anatase TiO_2 sample has a tetragonal structure. The energy band gap of the synthesized TiO_2 NPs was calculated 3.54 eV which was greater than that of the TiO_2 bulk with a band gap of 3.23 eV. The present work proves that Ir-doped TiO_2 NPs is a new technique using cheap precursors for photocatalytic degradation of CPs. This study provides a versatile approach for high-efficiency method for the degradation of toxic compounds of CPs such as 2-CP, 4-CP, 2,4-DCP and 2,4,6-TCP under solar irradiation in the presence of Ir-doped TiO_2 NPs as an outstanding photocatalyst. The overall degradation efficiencies for CPs under sunlight irradiation were found to be more than 70% within 60 min, that significantly enhanced by doping with Ir^{3+} ions. The increase in photocatalytic activity was due to the higher absorption and the 5d-electron transition of metal ions. Therefore Ir doping is effective for improving photocatalytic activity of TiO_2 for degradation of chlorinated pollutants under sunlight. In addition, the prepared Ir-doped TiO_2 NPs with various amounts (10µL to 50 µL) were screened for antimicrobial activity and revealed that the tested sample has an elevated antimicrobial activity.

ACKNOWLEDGEMENTS

The authors would like to acknowledge the Head, Department of Chemistry, Osmania University for providing the necessary facilities. The authors would like to thank DST-FIST, New Delhi, India for providing necessary analytical facilities in the department.

CONFLICT OF INTEREST

The authors declare that there is no conflict of interests regarding the publication of this paper.

REFERENCES

1. Liuxue Z, Xiulian W, Peng L, Zhixing S. Low temperature deposition of TiO2 thin films on polyvinyl alcohol fibers with photocatalytical and antibacterial activities. Applied Surface Science. 2008;254(6):1771-4.
2. He R-L, Wei Y, Cao W-B. Preparation of (Fe, N)-Doped TiO_2 Powders and Their Antibacterial Activities Under Visible Light Irradiation. Journal of Nanoscience and Nanotechnology. 2009;9(2):1094-7.
3. Erdural BK, Yurum A, Bakir U, Karakas G. Hydrothermal Synthesis of Nanostructured TiO_2 Particles and Characterization of Their Photocatalytic Antimicrobial Activity. Journal of Nanoscience and Nanotechnology. 2008;8(2):878-86.
4. Nicole C. Mueller BN. Exposure Modeling of Engineered

Nanoparticles in the Environment. Environmental Science & Technology. 2008;42(12):4447-53.
5. Gottschalk F, Ort C, Scholz RW, Nowack B. Engineered nanomaterials in rivers – Exposure scenarios for Switzerland at high spatial and temporal resolution. Environmental Pollution. 2011;159(12):3439-45.
6. Christine Ogilvie Robichaud AEU, Michael R. Darby, Lynne G. Zucker and Mark R. Wiesner. Estimates of Upper Bounds and Trends in Nano-TiO2Production As a Basis for Exposure Assessment. Environmental Science & Technology. 2009;43(12):4227-33.
7. Momeni MM, Hosseini MG. Photo-electrocatalytic activity of TiO2 nanotubes prepared with two-step anodization and treated under UV light irradiation. Nanochemistry Research. 2016;1(1):9-18.
8. Amini M, Ashrafi M. Photocatalytic degradation of some organic dyes under solar light irradiation using TiO2 and ZnO nanoparticles. Nanochemistry Research. 2016;1(1):79-86.
9. Haynes VN, Ward JE, Russell BJ, Agrios AG. Photocatalytic effects of titanium dioxide nanoparticles on aquatic organisms—Current knowledge and suggestions for future research. Aquatic Toxicology. 2017;185:138-48.
10. Chen Q, Yu Z, Pan Y, Zeng G, Shi H, Yang X, et al. Enhancing the photocatalytic and antibacterial property of polyvinylidene fluoride membrane by blending Ag–TiO2 nanocomposites. Journal of Materials Science: Materials in Electronics. 2017;28(4):3865-74.
11. Chong MN, Jin B, Chow CWK, Saint C. Recent developments in photocatalytic water treatment technology: A review. Water Research. 2010;44(10):2997-3027.
12. Daghrir R, Drogui P, Robert D. Modified TiO2 For Environmental Photocatalytic Applications: A Review. Industrial & Engineering Chemistry Research. 2013;52(10):3581-99.
13. Wang X-j, Yang W-y, Li F-t, Xue Y-b, Liu R-h, Hao Y-j. In Situ Microwave-Assisted Synthesis of Porous N-TiO2/g-C3N4 Heterojunctions with Enhanced Visible-Light Photocatalytic Properties. Industrial & Engineering Chemistry Research. 2013;52(48):17140-50.
14. Shangguan W, Yoshida A. Photocatalytic Hydrogen Evolution from Water on Nanocomposites Incorporating Cadmium Sulfide into the Interlayer. The Journal of Physical Chemistry B. 2002;106(47):12227-30.
15. Kumar SG, Devi LG. Review on Modified TiO2 Photocatalysis under UV/Visible Light: Selected Results and Related Mechanisms on Interfacial Charge Carrier Transfer Dynamics. The Journal of Physical Chemistry A. 2011;115(46):13211-41.
16. Zhu B-Z, Shan G-Q. Potential Mechanism for Pentachlorophenol-Induced Carcinogenicity: A Novel Mechanism for Metal-Independent Production of Hydroxyl Radicals. Chemical Research in Toxicology. 2009;22(6):969-77.
17. Zhu B-Z, Zhu J-G, Fan R-M, Mao L. Chapter One - Metal-Independent Pathways of Chlorinated Phenol/Quinone Toxicity. In: Fishbein JC, editor. Advances in Molecular Toxicology. 5: Elsevier; 2011. p. 1-43.
18. Gupta SS, Stadler M, Noser CA, Ghosh A, Steinhoff B, Lenoir D, et al. Rapid total destruction of chlorophenols by activated hydrogen peroxide. Science. 2002;296(5566):326-8.
19. Czaplicka M. Sources and transformations of chlorophenols in the natural environment. Science of The Total Environment. 2004;322(1):21-39.
20. Gou Y, Chen D, Su Z. Photocatalyst of nanometer TiO2/conjugated polymer complex employed for depigmentation of methyl orange. Applied Catalysis A: General. 2004;261(1):15-8.
21. Serpone N, Lawless D, Khairutdinov R. Size Effects on the Photophysical Properties of Colloidal Anatase TiO2 Particles: Size Quantization versus Direct Transitions in This Indirect Semiconductor? The Journal of Physical Chemistry. 1995;99(45):16646-54.
22. Gavade NL, Kadam AN, Gaikwad YB, Dhanavade MJ, Garadkar KM. Decoration of biogenic AgNPs on template free ZnO nanorods for sunlight driven photocatalytic detoxification of dyes and inhibition of bacteria. Journal of Materials Science: Materials in Electronics. 2016;27(10):11080-91.
23. García-Serrano J, Gómez-Hernández E, Ocampo-Fernández M, Pal U. Effect of Ag doping on the crystallization and phase transition of TiO2 nanoparticles. Current Applied Physics. 2009;9(5):1097-105.
24. Khade GV, Suwarnkar MB, Gavade NL, Garadkar KM. Green synthesis of TiO2 and its photocatalytic activity. Journal of Materials Science: Materials in Electronics. 2015;26(5):3309-15.
25. Kunze J, Ghicov A, Hildebrand H, Macak Jan M, Traveira L, Schmuki P. Challenges in the Surface Analytical Characterisation of Anodic TiO2 Films – a Review. Zeitschrift für Physikalische Chemie2005. p. 1561.
26. Pant HR, Pant B, Sharma RK, Amarjargal A, Kim HJ, Park CH, et al. Antibacterial and photocatalytic properties of Ag/TiO2/ZnO nano-flowers prepared by facile one-pot hydrothermal process. Ceramics International. 2013;39(2):1503-10.
27. Zhang J, Zhou P, Liu J, Yu J. New understanding of the difference of photocatalytic activity among anatase, rutile and brookite TiO2. Physical Chemistry Chemical Physics. 2014;16(38):20382-6.
28. Okada K, Yamamoto N, Kameshima Y, Yasumori A, MacKenzie KJ. Effect of Silica Additive on the Anatase-to-Rutile Phase Transition. Journal of the American Ceramic Society. 2001;84(7):1591-6.
29. Liu G, Yang HG, Wang X, Cheng L, Lu H, Wang L, et al. Enhanced Photoactivity of Oxygen-Deficient Anatase TiO2 Sheets with Dominant {001} Facets. The Journal of Physical Chemistry C. 2009;113(52):21784-8.
30. Wang J, Sun W, Zhang Z, Jiang Z, Wang X, Xu R, et al. Preparation of Fe-doped mixed crystal TiO2 catalyst and investigation of its sonocatalytic activity during degradation of azo fuchsine under ultrasonic irradiation. Journal of Colloid and Interface Science. 2008;320(1):202-9.
31. Sun X, Liu H, Dong J, Wei J, Zhang Y. Preparation and Characterization of Ce/N-Codoped TiO2 Particles for Production of H2 by Photocatalytic Splitting Water Under Visible Light. Catalysis Letters. 2010;135(3):219-25.
32. Gu L, Zhang X, Lei L. Degradation of Aqueous p-Nitrophenol by Ozonation Integrated with Activated Carbon. Industrial & Engineering Chemistry Research. 2008;47(18):6809-15.
33. RJ LS. Hazardous Chemicals Desk Reference. New York: John Wiley and Sons. ; 2002.
34. KD J. The fundamental and practice for the removal of phenolic compounds in wastewater. 1984.
35. Ph H. Handbook of Environmental Degradation Rates: Lewis Publishers; 1991.